Broadband Dual-Polarized Antenna Array with Endfire Radiation for 5G Mobile Phone Applications

Faizi Khajeim, Maryam; Moradi, Gholamreza; Shirazi, Reza Sarraf; Zhang, Shuai

Published in:
I E E E Antennas and Wireless Propagation Letters

DOI (link to publication from Publisher):
10.1109/LAWP.2021.3113993

Publication date:
2021

Document Version
Accepted author manuscript, peer reviewed version

Broadband Dual-Polarized Antenna Array for 5G Millimeter-Wave Handsets

Maryam Faizi Khajeim, Gholamreza Moradi, *Senior Member*, *IEEE,* Reza Sarraf Shirazi, Shuai Zhang, *Senior Member*, *IEEE*

***Abstract*—This letter presents a wideband compact dual-polarized antenna with end-fire radiation pattern for the fifth generation (5G) millimeter-wave (mm-wave) applications. The antenna achieves a –10 dB S_{11} bandwidth of 16.5 % (25-29.5 GHz). The antenna has a thickness of 1.6 mm and a clearance of 3.4 mm. The presented four-element array achieves a maximum realized gain of 9.9 dBi and 9.1 dBi for horizontal mode (H-mode) and vertical mode (V-mode), respectively. The antenna has a wide beamwidth in both elevation and azimuth planes with good scanning performance for both H-mode and V-mode.**

***Index Terms*—5G, dual-polarized, millimeter-wave, mobile antenna, phased array, substrate integrated waveguide (SIW).**

I. Introduction

In the last ten years, the millimeter-wave (mm-wave) technology has drawn considerable research interest for the fifth generation (5G) communication systems due to its capability of providing a high data rate, wide bandwidth, and low latency[1]. Several single polarized antennas have been reported in the literature [2]–[4]. Adopting dual-polarized antennas would increase channel capacity and reliability considerably. Several dual-polarized antennas for base stations of mm-wave band communication systems have been reported [5]–[7]. The large size of those antennas makes it difficult to be integrated into mobile devices. Dual polarized antennas for metal frame mobile phone applications have been reported [8]–[10]. Several dual-polarized antennas with a broadside radiation pattern have been reported [11], [12]. Antennas with end-fire radiation can provide a good tradeoff in terms of ease of integration, the performance of the antenna integrated inside the handset (with hand blockage), and user exposure [13]-[17]. To minimize the effect of the handset on the antenna's performance, a gap of 2 mm or more is required between the antenna and adjacent metallic components such as the screen [18]. The compact size, low complexity, easy integration, and low cost make the SIW-based end-fire antennas proper for millimeter-wave applications [19].

Several dual-polarized end-fire antennas have been reported in [13] and [20]–[24]. Designing an end-fire dual-polarized antenna with a wideband operating frequency band, compact size, and a good radiation pattern is still very challenging.

Manuscript received March 31, 2021; revised June 9, 2020; accepted July 7, 2020. Date of publication November 1, 2020; date of current version April 16, 2021. This work was supported by the AAU Young Talent Program. (Corresponding author: *Shuai Zhang*).

M. Faizi Khajeim, G. Moradi and R. Sarraf Shirazi are with the Microwave Measurement Research Laboratory, Department of Electrical Engineering, Amirkabir University of Technology (Tehran Polytechnic), Iran, Tehran 1591634311 (e-mail: mfaizi@aut.ac.ir; ghmoradi@aut.ac.ir; sarraf@aut.ac.ir).

S. Zhang is with the Department of Electronic Systems, Aalborg University, 9220 Aalborg, Denmark (e-mail: sz@es.aau.dk).

II. Antenna Design and Analysis

A. Antenna Structure

The configuration of the presented antenna array is shown in Fig. 1. The antenna is formed by a two-layer stack-up PCB (Sub. 1 and Sub. 2). The material of Sub.1 and Sub. 2 is Rogers RO4350B (ε_r = 3.66, tanδ = 0.0037) with a thickness of 0.762 mm and the prepreg is Rogers RO4450F (ε_r = 3.7, tanδ = 0.004) with a thickness of 0.1 mm. The thickness of all copper layers (M1, M2, and M3) is 18 μm.

A pair of U-shaped slots is etched in the top and bottom faces of the SIW and five matching pins (Via. 4) are inserted inside it to achieve wide operating bandwidth in the vertical mode (V-mode).

SIW antenna with U-shaped slots suffers from a narrow operating band. Inserting matching vias improves the operating bandwidth considerably [4]. Employing blind vias to increase the bandwidth would result in a multi-layer structure, which is not proper for integration with a horizontally polarized antenna. To decrease the cost and complexity of the structure through vias have been employed to increase the operating bandwidth using a thin single-layer structure.

A printed monopole antenna with a stripline feed is placed in front of the SIW aperture to perform a horizontally polarized antenna. Employing a dipole antenna in front of the SIW results in high cross-polarization, asymmetric radiation pattern, and a small scan range of V-mode [22]. The monopole antenna with parasitic elements employed in this work has a clearance of 1.7 mm. Therefore, there is enough space to etch slots on broad faces of SIW to achieve wide bandwidth. Moreover, there is no connection between the radiating part and the ground plane, which would result in low cross-polarization in the V-mode.

Four blind vias (Via. 1) are drilled from M1 to M2 to feed horizontal mode (H-mode). Via. 2 is drilled from M1 to M3 to excite V-mode inside the SIW. Connector. 1 and Connector. 2

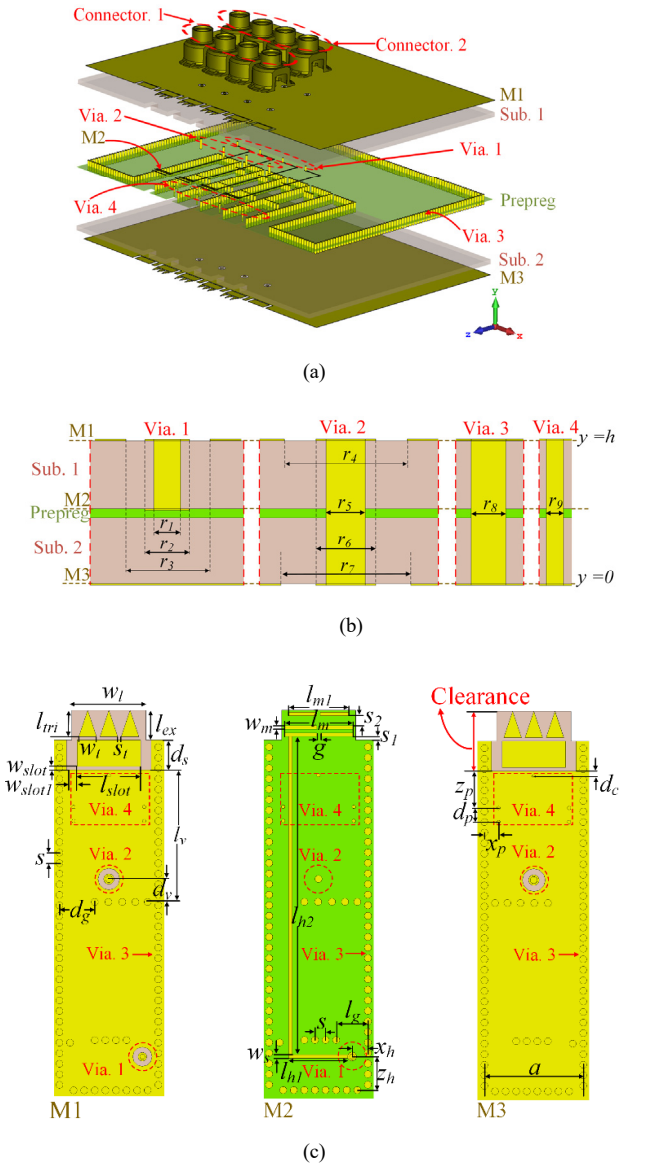

Fig. 1. Antenna configuration: (a) Exploded view, (b) Side view, (c) Dimensions and layers.

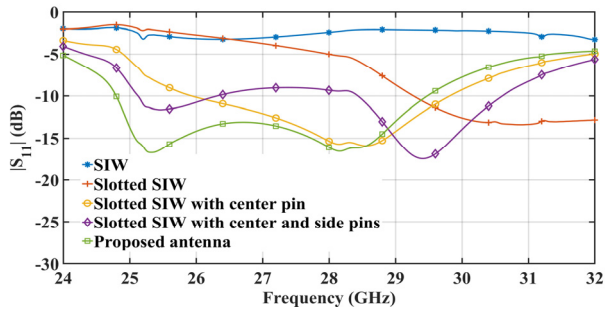

Fig. 2. The reflection coefficient of the presented single element and comparison with other configurations.

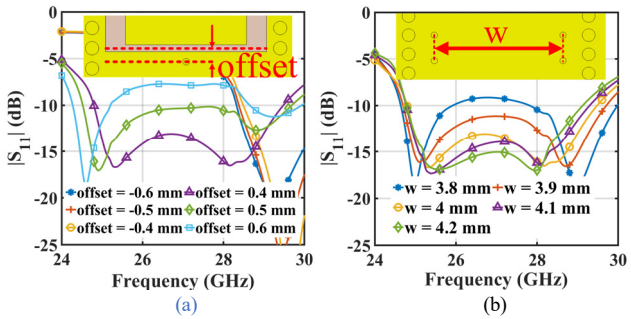

Fig. 3. The impact of the position of (a) center pin, and (b) side pins on the V-mode reflection coefficient.

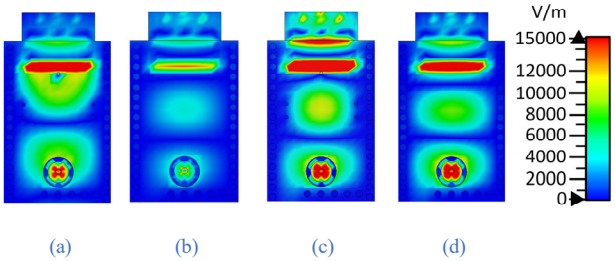

Fig. 4. The electric field distributions at 25.3 GHz (a) with, and (b) without matching pins, at 28.3 GHz (c) with, and (d) without matching pins.

are mounted on the M1 layer to feed vertical and horizontal modes, respectively. The horizontally polarized antenna and its feeding are placed in the middle plane of the SIW. Therefore, the H-mode does not affect the impedance matching of the V-mode. The optimized design parameters were: h = 1.624, w_l = 4.2, w_{slot} = 0.2, w_{slot1} = 0.6, w_t = 1, w_s = 0.2, w_m = 0.2, l_v = 7.5, l_{ex} = 1.7, l_{tri} = 1.5, l_g = 1.8, l_{h1} = 3.4, l_{h2} = 18.1, l_m = 3.8, l_{m1} = 3.4, l_{slot} = 4.8, s_t = 0.2, s = 0.6, s_1 = 0.2, s_2 = 0.6, a = 5.6, x_h = 0.9, z_h = 1.9, x_p = 0.8, z_p = 3.8, g = 0.2, d_p = 0.8, d_c = 0.3, d_g = 2, d_v = 1.4, d_s = 1.7, r_1 = 0.3, r_2 = 0.5, r_3 = 1.1, r_4 = 1.23, r_5 = 0.4, r_6 = 0.6, r_7 = 1.3, r_8 = 0.4, r_9 = 0.2 (all in millimeters).

B. Vertical Mode Analysis and Design

As illustrated in Fig. 2, Employing slots has improved impedance matching in frequencies larger than 29.5 GHz. Five pins (see via. 4 in Fig. 1) are inserted inside the SIW to improve impedance matching of the V-mode. A pin is inserted at the center of the SIW, which shifts the operating band to the target frequency band around 28 GHz. Inserting two pairs of pins symmetrically inside the SIW improves impedance matching. Employing triangular plates on the dielectric loading in front of the SIW tunes the real part of the input impedance and improves impedance matching.

To investigate the operation mechanism, a parametric analysis has been performed on the positions of matching pins (Via. 4 in Fig. 1). Fig. 3(a) and (b) demonstrate the impact of center and side pins' position on the impedance matching. Adding the pin in front of the slot (negative offset) does not have a noticeable impact on the reflection coefficient while placing the pin in the back of the slot (positive offset) improves the impedance matching significantly. Decreasing the offset makes two resonances closer to each other and improves impedance matching. The distance between side pins mainly affects the second resonance. Increasing the distance moves the second resonance to a lower frequency and

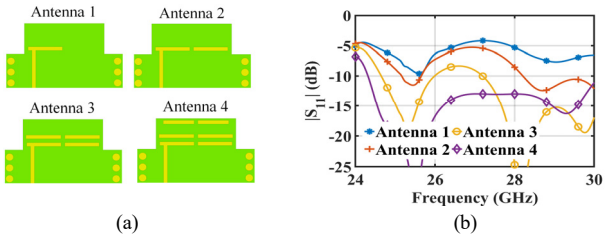

Fig. 5. (a) The design procedure of the H-mode, (b) The reflection coefficient comparison of different structures.

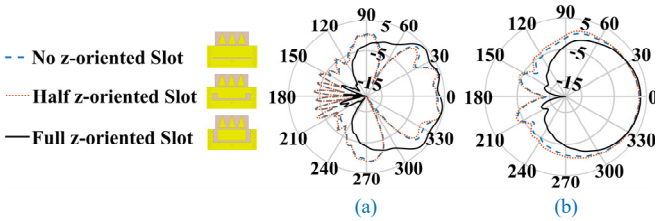

Fig. 6. The impact of the z-oriented slots on the radiation patterns in the (a) E-plane and (b) H-plane.

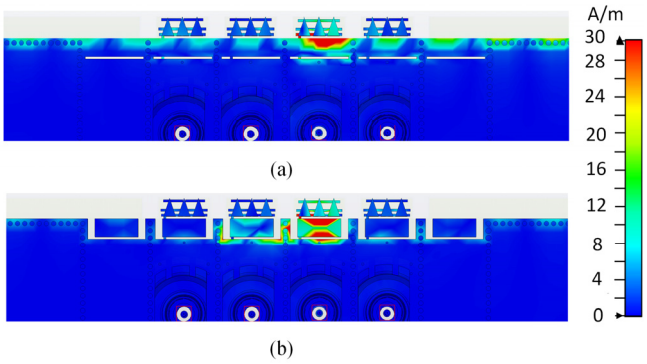

Fig. 7. The surface current distributions: (a) without z-oriented slots and (b) with z-oriented slots at 28 GHz.

improves the impedance matching in the middle of the frequency band.

The electric field distributions with and without pins are illustrated on the y=*h* plane in Fig. 4 in the resonance frequencies. Matching pins have increased the field amplitude around the SIW aperture and slots in both resonances, which confirms the advantages obtained by using matching pins. It can be realized that triangular plates mostly affect the field distribution in the second resonance.

C. Horizontal Mode Analysis and Design

The design procedure of the horizontally polarized antenna is shown in Fig. 5. A monopole-like antenna in front of the SIW aperture is used to support H-mode. As illustrated in Fig. 5(b), adding some parasitic rectangular strip elements would excite multi resonant modes, which leads to wide operating bandwidth. Fig. 6 demonstrates the performance advantages obtained by using the z-oriented slots in the ground plane. The surface current distribution on the M1 layer is presented in Fig. 7. In the H-mode without z-oriented slots, surface currents induced on the ground planes flow on the other elements of the array that leads to notches in the E-Plane

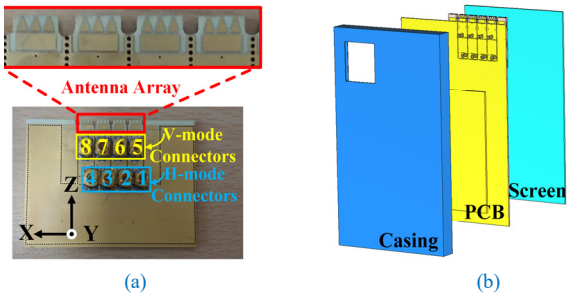

Fig. 8. (a) The fabricated antenna array. (b) Array inside the handset.

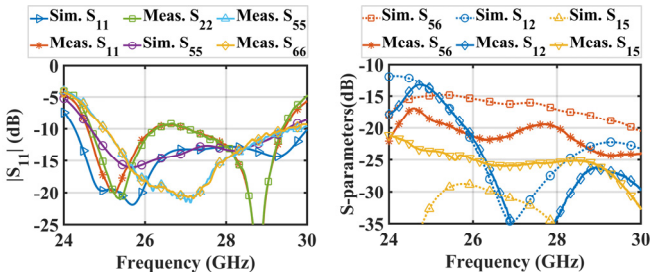

Fig. 9. The simulated and measured (a) reflection coefficients, and (b) mutual couplings of the presented antenna array.

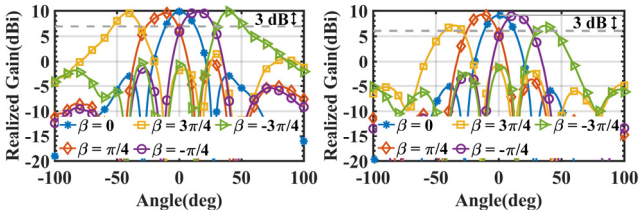

Fig. 10. The scanning performance of the presented antenna in the (a) H-mode, and (b) V-mode at 28 GHz.

radiation pattern. Moreover, the front-to-back radiation ratio has been increased by using full z-oriented slots.

III. Measurement Results

The fabricated 1×4 antenna array is demonstrated in Fig. 8(a). Fig. 8(b) depicts the antenna inside the handset. The antenna is placed on the top corner of the PCB, which is surrounded by the handset's plastic casing. The antenna is not covered by the screen. The measurements are performed in the anechoic chamber at Aalborg University. The simulated and measured reflection coefficients and mutual couplings are illustrated in Fig. 9(a) and (b), respectively. The measured operating band of V-mode and H-mode is 25-29.5 GHz and 24.7-29.5 GHz, respectively. The coupling between adjacent ports is less than -15 dB. The measured isolation between V-mode and H-mode ports is higher than 23 dB. The antenna array's ports are excited with equal magnitude and progressive phase shift of β. The simulated scanning performance is illustrated in Fig. 10. The angles of -44° to 44° are covered within the 3-dB beam scanning range for both V-mode and H-mode. Indeed, for H-mode, the 3-dB beam scanning range is

TABLE I
COMPARISON WITH OTHER DUAL-POLARIZED END-FIRE MM-WAVE ANTENNA ARRAYS

Ref No.	Pol.	Array Elements	BW (%)	Array Gain (dBi)	Number of Layers	Thickness	Clearance	Symmetrical Pattern	Scan Range
[13]	D-LP	2×4	28.6	H-mode: 10.5 V-mode: 11.6	1	0.12 λ_0	0.65 λ_0	Yes	NA
[21]	D-LP	1×4	19	H-mode: 9.27 V-mode: 9.16	4	0.19 λ_0	0.16 λ_0	No	-34° to 33°
[22]	D-LP	1×4	7	H-mode: 8.14 V-mode: 8.05	2	0.1 λ_0	0.25 λ_0	Yes	-42° to 39° (above 4 dBi)
[23]	D-LP	1×4	11.1	NA	3	0.23 λ_0	1.54 λ_0	No	NA
[24]	D-CP	1×4	22.5	12.8	2	0.37 λ_0	0.35 λ_0	Yes	±38°
This work	**D-LP**	**1×4**	**16.5**	**H-mode: 9.9 V-mode: 9.1**	**2**	**0.15 λ_0**	**0.3 λ_0**	**Yes**	**±44°**

D-LP: Dual-linear polarization D-CP: Dual-circular polarization NA: Not Available BW: Bandwidth

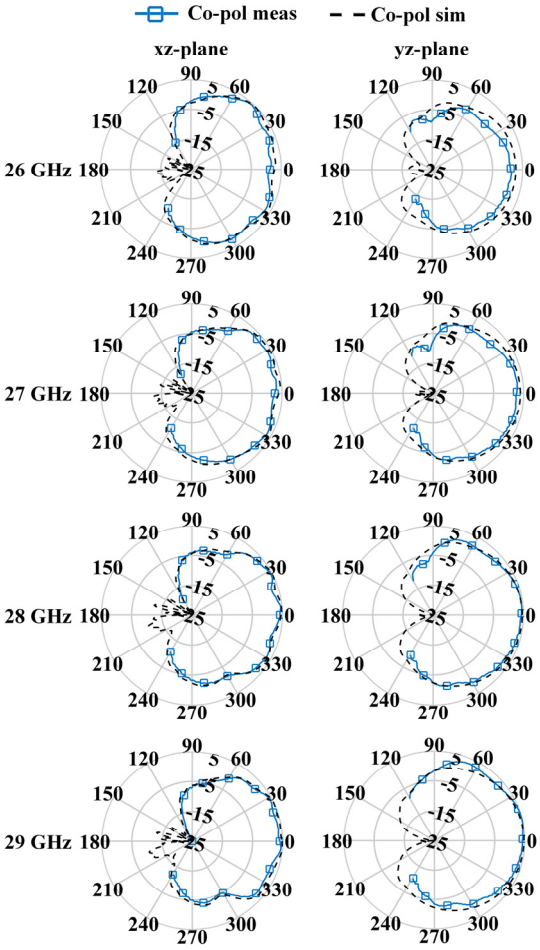

Fig. 11. The radiation patterns of the array element 1 in the H-mode.

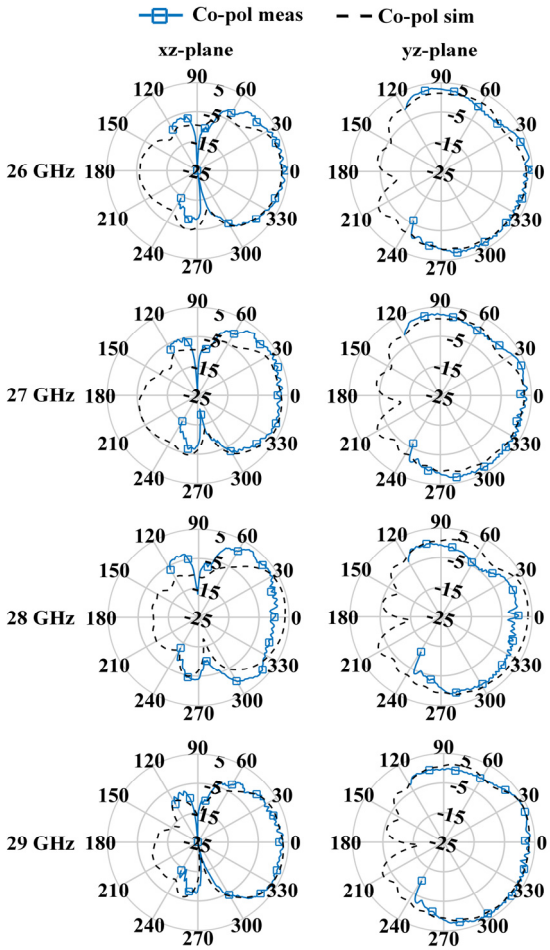

Fig. 12. The radiation patterns of the array element 5 in the V-mode.

from -52° to 52°. In the V-mode, the beamwidth is narrower than in the H-mode. Therefore, compared with the H-mode, the scanning capability of the V-mode is limited.

As illustrated in Fig. 11 and Fig. 12, the antenna has stable and symmetrical radiation patterns all over the operating band in both xz and yz-planes for both modes. The cross-polarization of the V-mode and H-mode is 18 dB and 13 dB lower than co-polarization, respectively, in both planes during the operating band.

Table I compares the performance of different mm-wave antennas. Compared with previously reported works, the presented antenna has a larger scanning range. The antenna has a small thickness, small clearance, and wide bandwidth simultaneously using a simple two-layer structure. The antenna has symmetrical radiation patterns in both planes for both V-mode and H-mode with low cross-polarization.

IV. CONCLUSION

A broadband dual-polarized antenna array for the 5G handset has been presented. A slotted SIW antenna is combined with a monopole-like antenna to achieve a dual-polarization feature. The good radiation performance, wide frequency bandwidth, and compact configuration make the presented antenna appropriate for 5G mobile phone devices.

REFERENCES

[1] W. Roh *et al.*, "Millimeter-wave beamforming as an enabling technology for 5G cellular communications: Theoretical feasibility and prototype results," *IEEE Commun. Mag.* vol. 52, no. 2, pp. 106-113, Feb. 2014.

[2] J. Wang, Y. Li, L. Ge, J. Wang, and K. M. Luk, "A 60 GHz horizontally polarized magnetoelectric dipole antenna array with 2-D multibeam endfire radiation," *IEEE Trans. Antennas Propagat.*, vol. 65, no. 11, pp. 5837-5845, Sep. 2017.

[3] S. Zhang, X. Chen, I. Syrytsin, and G.F. Pedersen, "A Planar switchable 3-D-coverage phased array antenna and its user effects for 28-GHz mobile terminal applications," *IEEE Trans. Antennas Propagat.*, vol. 65, no. 12, pp. 6413-6421, Dec. 2017.

[4] M. F. Khajeim, G. Moradi, R. S. Shirazi, S. Zhang, and G. F. Pedersen, "Wideband Vertically Polarized Antenna with Endfire Radiation for 5G Mobile Phone Applications," *IEEE Antennas Wireless Propag. Lett.*, vol. 19, no. 11, pp. 1948-1952, Nov. 2020.

[5] S. Hussain, S.W. Qu, W.L. Zhou, P. Zhang, and S. Yang, "Design and Fabrication of Wideband Dual-Polarized Dipole Array for 5G Wireless Systems," *IEEE Access*, vol. 8, pp. 65155-65163, Mar. 2020.

[6] B. Feng, X. He, and J.C. Cheng, "Dual-Wideband Dual-Polarized Metasurface Antenna Array for the 5G Millimeter Wave Communications Based on Characteristic Mode Theory," *IEEE Access*, vol. 8, pp. 21589-21601, Jan. 2020.

[7] B. Feng, Y. Tu, J. Chen, S. Yin, and K.L. Chung, "Dual Linearly-Polarized Antenna Array with High Gain and High Isolation for 5G Millimeter-Wave Applications," *IEEE Access*, vol. 8, pp. 82471-82480, Apr. 2020.

[8] R.M. Moreno, J. Ala-Laurinaho, A. Khripkov, J. Ilvonen, and V. Viikari, "Dual-Polarized mm-Wave Endfire Antenna for Mobile Devices," *IEEE Trans. Antennas Propagat*, vol. 68, no. 8, pp. 5924-5934, Aug. 2020.

[9] H. Li, Y. Cheng, L. Mei, and F. Wu, "Dual-Polarized Frame-Integrated Slot Arrays for 5G Mobile Handsets," *IEEE Antennas Wireless Propag. Lett.*, vol. 19, no. 11, pp. 1953-1957, Nov. 2020.

[10] R.M. Moreno, J. Kurvinen, J. Ala-Laurinaho, A. Khripkov, J. Ilvonen, J. van Wonterghem, and V. Viikari, "Dual-polarized mm-wave endfire chain-slot antenna for mobile devices," *IEEE Trans. Antennas Propagat*, vol. 69, no. 1, pp. 25-34, Jun. 2020.

[11] S. Liao, and Q. Xue, "Dual polarized planar aperture antenna on LTCC for 60-GHz antenna-in-package applications," *IEEE Trans. Antennas Propagat.*, vol. 65, no. 1, pp. 63-70, Jan. 2017.

[12] Y. Li, and K. M. Luk, "60-GHz dual-polarized two-dimensional switch-beam wideband antenna array of magneto-electric dipoles," *in Proc. IEEE Int. Symp. Antennas Propag. USNC/URSI Nat. Radio Sci. Meeting*, pp. 1542-1543, Jul. 2015.

[13] A. Li, and K.M. Luk, "Single-Layer Wideband End-Fire Dual-Polarized Antenna Array for Device-to-Device Communication in 5G Wireless Systems," *IEEE Trans. Vehicular Tech.*, vol. 69, no. 5, pp. 5142-5150, May 2020.

[14] Y. Li, and K.M. Luk, "A multibeam end-fire magnetoelectric dipole antenna array for millimeter-wave applications," *IEEE Trans. Antennas Propagat*, vol. 64, no. 7, pp. 2894-2904, Apr. 2016.

[15] V. Raghavan, M.L. Chi, M.A. Tassoudji, O.H. Koymen, and J. Li, "Antenna placement and performance tradeoffs with hand blockage in millimeter wave systems," *IEEE Trans. Communications*, vol. 67, no. 4, pp. 3082-3096, Apr. 2019.

[16] J. Helander, K. Zhao, Z. Ying, and D. Sjöberg, "Performance analysis of millimeter-wave phased array antennas in cellular handsets," *IEEE Antennas Wireless Propag. Lett.*, vol. 15, pp. 504-507, Jul. 2015.

[17] A.R. Guraliuc, M. Zhadobov, R. Sauleau, L. Marnat, and L. Dussopt, "Near-field user exposure in forthcoming 5G scenarios in the 60 GHz band," *IEEE Trans. Antennas Propagat*, vol. 65, no. 12, pp. 6606-6615, Nov. 2017.

[18] I.J. Hwang, B. Ahn, S.C. Chae, J.W. Yu, and W.W. Lee, "Quasi-Yagi antenna array with modified folded dipole driver for mmWave 5G cellular devices," *IEEE Antennas Wireless Propag. Lett.*, vol. 18, no. 5, pp. 971-975, Mar. 2019.

[19] Y. Cao, Y. Cai, L. Wang, Z. Qian and L. Zhu, "A review of substrate integrated waveguide end-fire antennas," *IEEE Access*, vol. 6, pp. 66243-66253, Nov. 2018.

[20] A. Li, K.M. Luk, and Y. Li, "A dual linearly polarized end-fire antenna array for the 5G applications," *IEEE Access*, vol. 6, pp. 78276-78285, Dec. 2018.

[21] H. Li, Y. Li, L. Chang, W. Sun, X. Qin, and H. Wang, "A Wideband Dual-Polarized Endfire Antenna Array With Overlapped Apertures and Small Clearance for 5G Millimeter-Wave Applications," *IEEE Trans. Antennas Propagat*, vol. 69, no. 2, pp. 815-824, Feb. 2021.

[22] J. Zhang, K. Zhao, L. Wang, S. Zhang, and G.F. Pedersen, "Dual-Polarized Phased Array with End-Fire Radiation for 5G Handset Applications," *IEEE Trans. Antennas Propagat.*, vol. 68, no. 4, pp. 3277-3282. Apr. 2020.

[23] Y.W. Hsu, T.C. Huang, H.S. Lin, and Y.C. Lin, "Dual-polarized quasi Yagi–Uda antennas with endfire radiation for millimeter-wave MIMO terminals," *IEEE Trans. Antennas Propagat.*, vol. 65, no. 12, pp. 6282-6289, Dec. 2017.

[24] Q. Wu, J. Hirokawa, J. Yin, C. Yu, H. Wang and W. Hong, "Millimeter-Wave Multibeam Endfire Dual-Circularly Polarized Antenna Array for 5G Wireless Applications," *IEEE Trans. Antennas Propag.*, vol. 66, no. 9, pp. 4930-4935, Sept. 2018.